Effects of Proline Mutations on the Folding of Staphylococcal Nuclease †

ARTICLE *in* BIOCHEMISTRY · MARCH 1999

Impact Factor: 3.02 · DOI: 10.1021/bi981962+ · Source: PubMed

Effects of Proline Mutations on the Folding of Staphylococcal Nuclease[†]

Kosuke Maki,[‡] Teikichi Ikura,[‡] Toshiya Hayano,[§] Nobuhiro Takahashi,[||] and Kunihiro Kuwajima*[,‡]

Department of Physics, School of Science, University of Tokyo, 7-3-1 Hongo, Bunkyo-ku, Tokyo 113-0033, Japan, Corporate Research and Development Laboratory, Tonen K.K., 1-3-1 Nishi-tsurugaoka, Ohi-machi, Iruma-gun, Saitama 356-8505, Japan, and Tokyo University of Agriculture and Technology, 3-5-8 Saiwai-cho, Fuchu-shi, Tokyo 183-8509, Japan

Received August 17, 1998; Revised Manuscript Received November 23, 1998

ABSTRACT: Effects of proline isomerizations on the equilibrium unfolding and kinetic refolding of staphylococcal nuclease were studied by circular dichroism in the peptide region (225 nm) and fluorescence spectra of a tryptophan residue. For this purpose, four single mutants (P11A, P31A, P42A, and P56A) and four multiple mutants (P11A/P47T/P117G, P11A/P31A/P47T/P117G, P11A/P31A/P42A/P47T/P117G, and P11A/P31A/P42A/P47T/P56A/P117G) were constructed. These mutants, together with the single and double mutants for Pro^{47} and Pro^{117} constructed in our previous study, cover all six proline sites of the nuclease. The P11A, P31A, and P42A mutations did not change the stability of the protein remarkably, while the P56A mutation increased protein stability to a small extent by 0.5 kcal/mol. The refolding kinetics of the protein were, however, affected remarkably by three of the mutations, namely, P11A, P31A, and P56A. Most notably, the amplitude of the slow phase of the triphasic refolding kinetics of the nuclease observed by stopped-flow circular dichroism decreased by increasing the number of the proline mutations; the slow phase disappeared completely in the proline-free mutant (P11A/P31A/P42A/P47T/P56A/P117G). The kinetic refolding reactions of the wild-type protein assessed in the presence of *Escherichia coli* cyclophilin A showed that the slow phase was accelerated by cyclophilin, indicating that the slow phase was rate-limited by cis−trans isomerization of the proline residues. Although the fast and middle phases of the refolding kinetics were not affected by cyclophilin, the amplitude of the middle phase decreased when the number of the proline mutations increased; the percent amplitudes for the wild-type protein and the proline-free mutants were 43 and 13%, respectively. In addition to these three phases detected with stopped-flow circular dichroism, a very fast phase of refolding was observed with stopped-flow fluorescence, which had a shorter dead time (3.6 ms) than the stopped-flow circular dichroism. The following conclusions were drawn. (1) The effects of the P11A, P31A, and P56A mutations on the refolding kinetics indicate that the isomerizations of the three proline residues are rate-limiting, suggesting that the structures around these residues (Pro^{11}, Pro^{31}, and Pro^{56}) may be organized at an early stage of refolding. (2) The fast phase corresponds to the refolding of the native proline isomer, and the middle phase whose amplitude has decreased when the number of proline mutations was increased may correspond to the slow refolding of non-native proline isomers. The occurrence of the fast- and slow-refolding reactions together with the slow phase rate-limited by the proline isomerization suggests that there are parallel folding pathways for the native and non-native proline isomers. (3) The middle phase did not completely disappear in the proline-free mutant. This suggests that the slow-folding isomer is produced not only by the proline isomerizations but also by another conformational event that is not related to the prolines. (4) The very fast phase detected with the fluorescent measurements suggests that there is an intermediate at a very early stage of kinetic refolding.

The understanding of the mechanism of protein folding has remarkably progressed during the past decade. Many globular proteins have been found to accumulate intermediate states during refolding from the unfolded (U) state to the native (N) state. The structure of these intermediates has been characterized in detail (*1*−*10*). However, certain globular proteins show complex multiphasic refolding kinetics that are not directly related to the accumulation of the folding intermediates; the complex folding kinetics of these proteins have often been interpreted in terms of the heterogeneity of the U state. In most cases, the heterogeneity of the U state arises from the isomerizations of X−Pro peptide bonds in proline-containing proteins (*2*, *11*−*21*). Proline isomerization is a slower reaction than folding. Therefore, the isomerization to a native proline isomer in the U state is occasionally rate-limiting, and more often, the heterogeneity of the U state leads to multiple folding parallel pathways. Although the isomerization of an X−Pro peptide bond is itself different from folding, it is important to assign the individual isomerization events to the observed folding kinetics. This

[†] This work was supported by Grants-in-Aids for Scientific Research from the Ministry of Education, Science and Culture of Japan.

* To whom correspondence should be addressed.
[‡] University of Tokyo.
[§] Tonen K.K.
[||] Tokyo University of Agriculture and Technology.

10.1021/bi981962+ CCC: $18.00
Published on Web 01/29/1999

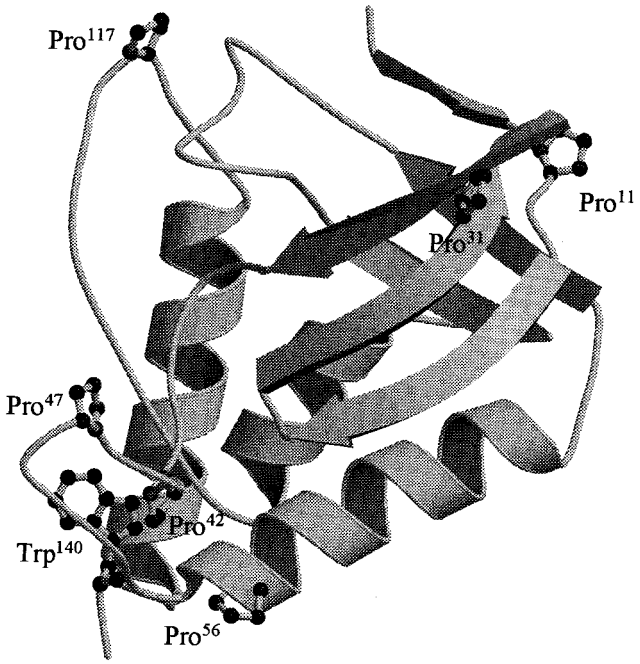

FIGURE 1: X-ray crystal structure of wild-type SNase. The six proline residues and Trp^{140} are shown explicitly. The drawing was generated using the program MOLSCRIPT (*46*).

is because the isomerization of an X−Pro peptide bond is a significant process in both in vitro and in vivo folding reactions.

Staphylococcal nuclease (SNase)[1] is a small globular protein of 149 amino acid residues (*22*). SNase lacks both disulfide bonds and cysteine residues. Its high-resolution X-ray crystal structure is available (Figure 1); it contains three helices and a five-stranded β-barrel (*23*, *24*). This protein shows multiphasic kinetics of folding; there are at least three (fast, middle, and slow) phases of refolding kinetics under the present conditions (pH 7.0 and 20 °C). SNase contains six proline residues (Pro^{11}, Pro^{31}, Pro^{42}, Pro^{47}, Pro^{56}, and Pro^{117}) (*22*). The X−Pro peptide bonds of Pro^{11}, Pro^{31}, Pro^{42}, and Pro^{56} are in the trans form in the N state (see Figure 1), while the X−Pro peptide bonds of Pro^{47} and Pro^{117} can be either in the trans form or in the cis form (*25*, *26*). Thus, the isomerization of some of the six X−Pro peptide bonds of the protein may be responsible for the multiphasic folding kinetics (*27*−*30*). In fact, recently, Walkenhorst et al. (*31*) have shown that the slow phase of the kinetic refolding disappears in the Pro-minus mutant in which all six proline residues of SNase are replaced by other amino acids. However, the contributions of the individual X−Pro bonds to the folding of this protein are not yet fully understood.

We have previously studied the effects of isomerizations of Pro^{47} and Pro^{117} on the stability and the folding of SNase with circular dichroism (CD), absorption spectroscopy, and molecular dynamics simulation (*30*). To study the effect of isomerization, we constructed SNase mutants (P47A, P47T, P117G, and P47T/P117G). It has been shown that the P47A and P47T mutations cause no changes in the stability, nor do these mutations affect folding kinetics. Molecular dynamics simulations have shown that the loop region, where Pro^{47} is located, is highly flexible. The isomerization of the His^{46}−Pro^{47} peptide bond is therefore expected to have no effect on the folding reaction of the SNase molecule. On the other hand, the P117G mutation increased stability and changed both the folding and unfolding kinetics of SNase (*30*). However, the P47T/P117G double mutant still exhibits multiphasic kinetics with the slow phase that are known to be absent in the Pro-minus mutant (*31*); apparently there are at least four phases in the refolding of P47T/P117G at pH 7.0 and 20 °C. Therefore, other proline residues must be responsible for the multiphasic behavior of SNase folding.

In this study, we first investigated the isomerizations of Pro^{11}, Pro^{31}, Pro^{42}, and Pro^{56} to determine their roles in the folding of SNase. To study the role of these isomerizations in the folding of SNase, we constructed four new single mutants of SNase (P11A, P31A, P42A, and P56A) and four multiple mutants of SNase [P11A/P47T/P117G, P11A/P31A/P47T/P117G (P42P56), P11A/P31A/P42A/P47T/P117G (P56), and P11A/P31A/P42A/P47T/P56A/P117G (Pro^-)]. Equilibrium and kinetic CD measurements were used to study the equilibrium unfolding and the kinetic refolding of wild-type SNase, the four single mutants, the P47T/P117G mutant constructed previously, and the above four multiple mutants. The refolding of wild-type SNase in the presence of *Escherichia coli* cyclophilin A (CyPA) was then considered. Because CyPA has peptidyl prolyl *cis*−*trans* isomerase (PPIase) activity, the effect of CyPA on the refolding kinetics provides information about which phases of the multiphasic refolding are rate-limited by proline isomerization (*32*, *33*). The kinetic refolding of Pro^- was also studied by intrinsic tryptophan fluorescence for the purpose of investigating a very early stage of refolding kinetics. This very early stage is more brief than the fast phase of the refolding but important for fully understanding the overall folding process.

The effects of isomerization of individual proline residues on kinetic refolding were found to be remarkably different. This study shows that isomerizations of the proline residues (Pro^{11}, Pro^{31}, and Pro^{56}) that are involved in a hydrophobic core formed by a five-stranded β-barrel and helix 1 are rate-limiting and are responsible for the slow phase of refolding. On the other hand, the isomerizations of the proline residues (Pro^{42} and Pro^{47}) that are close to or within a flexible loop (residue 43−53) are not responsible for the slow phase of refolding. These results also show that not only the slow phase but also the middle phase of refolding is associated with proline residues. However, in contrast to the slow phase, the middle phase is not rate-limited by proline isomerization. The relationship of these results to the mechanism of SNase folding will be considered in the Discussion.

MATERIALS AND METHODS

Chemicals. A specially prepared reagent grade urea for biochemical use was purchased from Nacalai Tesque Inc. (Kyoto, Japan). The urea stock solution was deionized with a mixed-bed column of Amberlite IR-120B and IRA-402 for removal of cyanate and ammonium ions. Cyanate in

[1] Abbreviations: SNase, staphylococcal nuclease; CD, circular dichroism; P42P56, P11A/P31A/P47T/P117G; P56, P11A/P31A/P42A/P47T/P117G; Pro^-, P11A/P31A/P42A/P47T/P56A/P117G; CyPA, cyclophilin A; PPIase, peptidyl prolyl *cis*−*trans* isomerase; EDTA, ethylenediamine-*N*,*N*,*N*′,*N*′-tetraacetic acid; DNase I, deoxyribonuclease I; DTT, dithiothreitol; EGTA, [ethylenebis(oxyethylenenitrilo)]tetraacetic acid.

particular is known to modify the amino groups of proteins (*34*). The urea solutions were used within several days. An Atago 3T refractometer was used to determine the concentration of urea with a refractive index of 589 nm (*34*). All other chemicals were either specially prepared or guaranteed reagent-grade chemicals.

Single and Multiple Mutants of SNase. The expression plasmids of single and multiple mutants of SNase were constructed from pMT7-SN and pMT7-SN-P47T/P117G (*30*), respectively, using the Kunkel method, employing a MUTA-GENE phagemid in vitro mutagenesis kit (Bio-Rad) (*35*). Both pMT7-SN and pMT7-SN-P47T/P117G involve a promoter for T7 RNA polymerase to overexpress the proteins (*36*) and an intergenic region of phage M13 DNA. All the sequences of the genes of the single and multiple mutants of SNase were identified by an ALF express autosequencer (Pharmacia).

Purifications of Single and Multiple Mutants of SNase. The single and multiple mutants of SNase were purified by methods reported previously (*30*), albeit with a small modification. The cells containing the protein were lysed by sonication in a buffer containing 50 mM Tris-HCl, 1 mM ethylenediamine-*N*,*N*,*N*′,*N*′-tetraacetic acid (EDTA), 100 mM sodium chloride, and 133 μM phenylmethanesulfonyl fluoride (pH 8.0). The supernatant was collected, to which deoxyribonuclease I (DNase I) and $MgCl_2$ were added so that the concentrations of DNase I and $MgCl_2$ were 0.1 mg/mL and 2 mM, respectively. After the protein solution was incubated for 1 h at room temperature, ammonium sulfate was added to 35% saturation and further ammonium sulfate was added to the supernatant to reach 80% saturation. The precipitate by the ammonium sulfate fractionation was dissolved in a buffer containing 100 mM ammonium acetate, 10 mM dithiothreitol (DTT), and 6 M guanidine hydrochloride (pH 8.0) to completely dissolve the protein. The protein solution was loaded onto a Sephacryl S-100 column equilibrated with a 100 mM ammonium acetate buffer (pH 8.0). The fractions containing the protein were collected and then passed through a fast-flow S Sepharose column equilibrated with a 50 mM Tris-HCl buffer (pH 8.0). The column was eluted with a linear gradient of sodium chloride to a final concentration of 1 M. The purified protein solution was again applied to a Sephacryl S-100 column equilibrated with a 100 mM ammonium acetate buffer (pH 8.0), which was then followed by lyophilization. The concentrations of wild-type SNase and all of the mutants used were determined spectrophotometrically using an extinction coefficient, $E^{1\%}_{1cm}$, of 9.3 at 280 nm (*22*).

Purification of CyPA. E. coli (HB101) cells carrying the genes of CyPA on a plasmid pATtrpEPPIb were described previously (*37*). CyPA was purified with a previously described method (*38*).

Sample Preparation for Equilibrium Measurements. The lyophilized protein was dissolved in a buffer containing 50 mM sodium cacodylate, 50 mM sodium chloride, 1 mM [ethylenebis(oxyethylenenitrilo)]tetraacetic acid (EGTA), and a high concentration of urea (typically 8 M) (pH 7.0). A high concentration of urea is necessary for the protein molecules to be monomeric. After filtration through a Millipore membrane filter (MILLEX-HV) with a pore size of 0.45 μm, the protein solution was passed through a Sephadex G-25 column (NAP-25, Pharmacia) equilibrated with 50 mM sodium cacodylate, 50 mM sodium chloride, and 1 mM EGTA. The sample solutions for equilibrium measurement were prepared by diluting the protein solution thus prepared with the same buffer containing an appropriate concentration of urea. The concentrations of wild-type SNase and all mutants used were 0.3−0.5 mg/mL.

Sample Preparation for Kinetic Measurements. The refolding buffer solution for kinetic measurements in the absence of CyPA contained 50 mM sodium cacodylate, 50 mM sodium chloride, and 1 mM EGTA. The solution for measurements in the presence of CyPA contained 25 mM phosphate, 50 mM sodium chloride, 1 mM EGTA, and 1 mM DTT. The lyophilized protein was dissolved in a buffer solution that contained 4.5 M urea (pH 7.0) for refolding, which was induced by a urea concentration jump (4.5 to 0.39 M). Another method of dissolving the lyophilized protein included a pH 1.8 solution, which induced refolding by causing a jump in the pH. The protein solutions were filtered through a membrane filter (MILLEX, pore size of 0.45 μm) and degassed before measurements. Refolding was initiated by stopped-flow mixing of the unfolded protein solution and the refolding buffer solution. CyPA was contained in the refolding buffer when the extent of refolding was measured in the presence of CyPA. The pH of the refolding buffer for the pH jump was adjusted so that the final pH was 5.9 or 6.6. The final pH value of 5.9 was chosen because it was useful in reducing the rate of refolding for detecting the very fast phase. The concentrations of wild-type SNase and all of the mutants of SNase were 0.1 mg/mL for the kinetic CD measurements and 0.01 and 0.1 mg/mL for the kinetic fluorescence measurements, respectively.

Measurement. All measurements were carried out at 20 °C with circulating water. Equilibrium CD spectra were obtained with a Jasco J-720 spectropolarimeter. The mean residue ellipticity was calculated by taking 113 as the mean residue weight of SNase (*22*). The path lengths of the sample cells for the equilibrium measurements were 1.00 and 10.0 mm for the far- and near-UV regions, respectively. Kinetic CD measurements were carried out using a stopped-flow apparatus (specially constructed by Unisok, Inc., Osaka, Japan) with a dead time of 23 ms. The apparatus was attached to the above spectropolarimeter (*39*, *40*). The path length and the mixing ratio of the stopped-flow apparatus were 3.8 mm and 1:10.4, respectively. Kinetic fluorescence measurements were carried out using a stopped-flow fluorometer, which was specially designed and constructed by Unisok, Inc. This fluorometer has a dead time of 3.6 ms. The refolding reaction was assessed by monitoring time-dependent changes of the tryptophan fluorescence intensity of the protein. The excitation wavelength was 295 nm. The emission light above 320 nm, obtained with an SC32 high-pass filter which cut off the light below 320 nm, was detected. The path length and mixing ratio were 2 mm and 1:9.7, respectively.

RESULTS

CD Spectra of Wild-Type and Mutant SNase. Figures 2a,b and 3a,b show the far- and near-UV CD spectra of wild-type SNase, its four single mutants (P11A, P31A, P42A, and P56A), and its four multiple mutants (P11A/P47T/P117G, P42P56, P56, and Pro$^-$) in the native (N) state in the absence

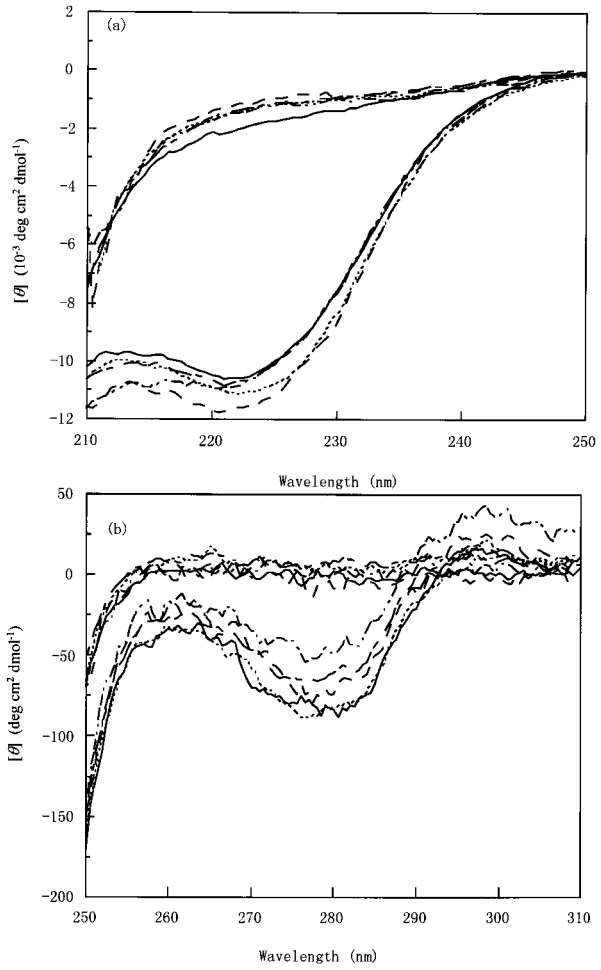

FIGURE 2: Far- and near-UV CD spectra of wild-type SNase and its four single mutants in the N state, in the absence of urea, and in the U state, in the presence of 7 M urea, at pH 7.0 and 20 °C (50 mM sodium cacodylate, 50 mM sodium chloride, and 1 mM EGTA). (a) The far-UV CD spectra of wild-type SNase (solid line), P11A (dotted line), P31A (dashed line), P42A (dot−dash line), and P56A (double dot−dash line) in the N state (thin lines) and in the U state (thick lines). (b) The near-UV CD spectra of wild-type SNase (solid line), P11A (dotted line), P31A (dashed line), P42A (dot−dash line), and P56A (double dot−dash line) in the N state (thin lines) and in the U state (thick lines).

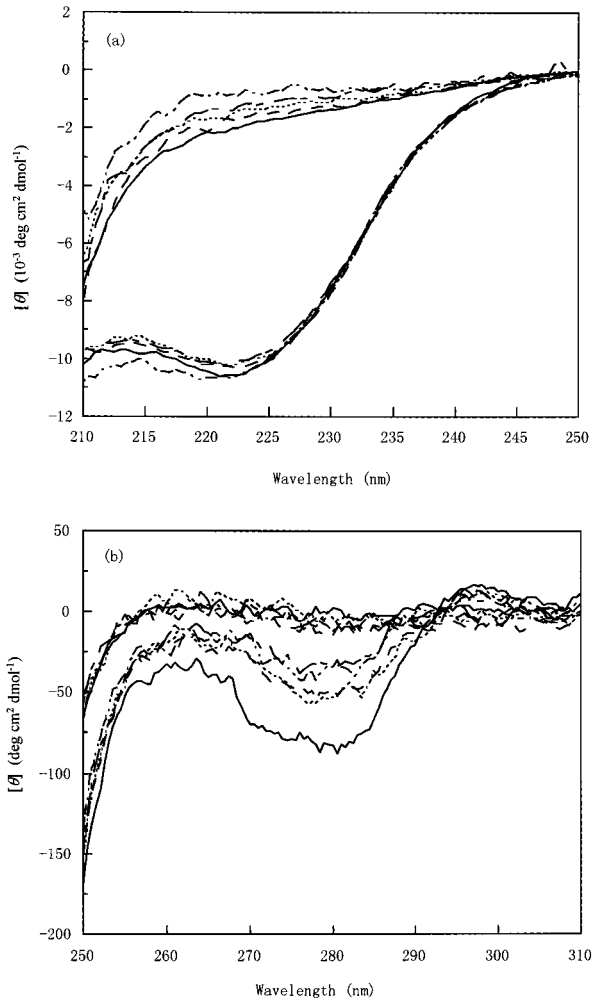

FIGURE 3: Far- and near-UV CD spectra of wild-type SNase and its four multiple mutants in the N state, in the absence of urea, and in the U state, in the presence of 7 M urea at pH 7.0 and 20 °C (50 mM sodium cacodylate, 50 mM sodium chloride, and 1 mM EGTA). (a) The far-UV CD spectra of wild-type SNase (solid line), P11A/P47T/P117G (dotted line), P42P56 (dashed line), P56 (dot−dash line), and Pro$^-$ (double dot−dash line) in the N state (thin lines) and in the U state (thick lines). (b) The near-UV CD spectra of wild-type SNase (solid line), P11A/P47T/P117G (dotted line), P42P56 (dashed line), P56 (dot−dash line), and Pro$^-$ (double dot−dash line) in the N state (thin lines) and in the U state (thick lines).

of urea and in the fully unfolded (U) state in 7 M urea at pH 7.0 (50 mM sodium cacodylate, 50 mM sodium chloride, and 1 mM EGTA) and 20 °C. The amino acid substitutions for the proline residues more strongly affect the near-UV spectra than the far-UV ones. In addition, the multiple substitutions tend to decrease the CD intensity in the near-UV region more remarkably than single substitutions. These changes in the CD spectra may arise from changes in the environment of aromatic (tyrosyl) residues without unfolding the protein molecule. The equilibrium unfolding reactions of the SNase mutants have shown that neither the N state stability nor the cooperativity of the unfolding transition is extensively changed by the proline mutations, indicating that the mutants are fully in the N state in the absence of urea (see below).

Equilibrium Unfolding. The transition curves of the urea-induced unfolding of the wild-type protein, the four single mutants (P11A, P31A, P42A, and P56A), and the four multiple mutants of SNase (P11A/P47T/P117G, P42P56, P56, and Pro$^-$) were obtained with the CD measurement at 225 and 276 nm, at pH 7.0 (50 mM sodium cacodylate, 50 mM sodium chloride, and 1 mM EGTA) and 20 °C. These curves obtained from the CD ellipticity at 225 nm and expressed in terms of the apparent fractional extent, F_{app}, of unfolding for wild-type and mutant SNase are illustrated in Figures 4 and 5. The F_{app} values were obtained with eq 1 from the observed CD ellipticity, $\theta_{obs}(C)$, at a concentration of urea, C, and the ellipticity values, θ_N and θ_U, in the N and U states, respectively, as

$$F_{app}(C) = \frac{\theta_{obs}(C) - \theta_N}{\theta_U - \theta_N} \quad (1)$$

Both θ_N and θ_U are assumed to be linearly dependent on C and are given by $\theta_N = \theta_{N_1} + \theta_{N_2}C$ and $\theta_U = \theta_{U_1} + \theta_{U_2}C$, respectively. The transition curve of P117G was identical to the curve of P47T/P117G shown in the previous study (*30*). The transition curves measured at the different wavelengths were found to be coincident with each other,

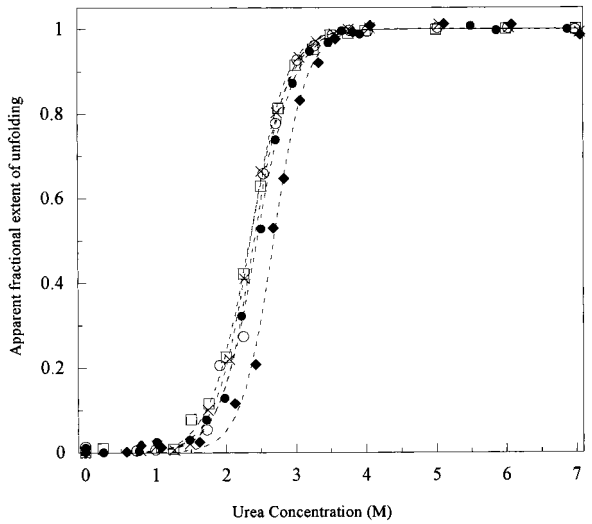

FIGURE 4: Equilibrium unfolding transition curves of wild-type SNase and its four single mutants at pH 7.0 and 20 °C, monitored by CD at 225 nm (50 mM sodium cacodylate, 50 mM sodium chloride, and 1 mM EGTA). The apparent extent of unfolding for wild-type SNase (●), P11A (×), P31A (□), P42A (○), and P56A (◆) at each urea concentration is plotted. Broken lines show the equilibrium unfolding transition curves obtained by nonlinear least-squares fitting of the data.

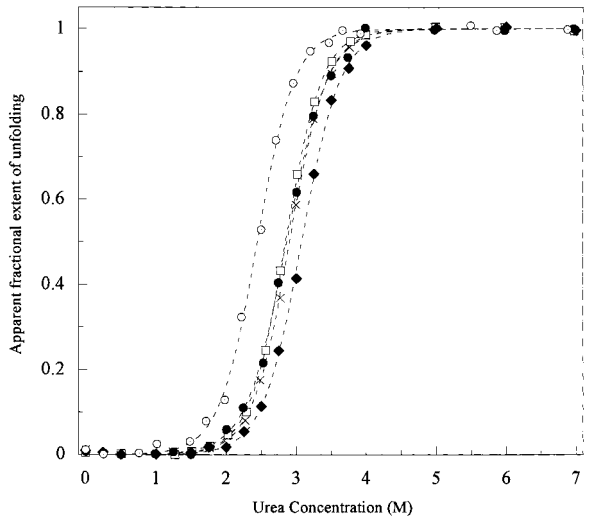

FIGURE 5: Equilibrium unfolding transition curves of wild-type SNase and its four multiple mutants at pH 7.0 and 20 °C, monitored by CD at 225 nm (50 mM sodium cacodylate, 50 mM sodium chloride, and 1 mM EGTA). The apparent extent of unfolding for wild-type SNase (○), P11A/P47T/P117G (×), P42P56 (□), P56 (●), and Pro$^-$ (◆) at each urea concentration is plotted. Broken lines show the equilibrium unfolding transition curves obtained by nonlinear least-squares fitting of the data.

suggesting the two-state mechanism of the unfolding transition for wild-type and mutant SNase.

Equilibrium unfolding parameters of the transition curves of Figures 4 and 5 were calculated on the basis of the two-state approximation, in which only the N and U states were assumed to be populated in the transition zone as

$$N \rightleftharpoons^{K_U} U$$

where K_U is the apparent equilibrium constant, and is related to the free energy change of unfolding, ΔG_U, given by

$$K_U = \exp\left(-\frac{\Delta G_U}{RT}\right) \quad (2)$$

where R and T are the gas constant and absolute temperature, respectively. For many globular proteins, ΔG_U is known to be well approximated as a linear function of C, so that

$$\Delta G_U = \Delta G_U^{H_2O} - mC \quad (3)$$

where $\Delta G_U^{H_2O}$ is the ΔG_U extrapolated at 0 M urea and m is the dependence of ΔG_U on C, and represents a cooperativity index for the unfolding transition. In the two-state approximation, the F_{app} is related to $\Delta G_U^{H_2O}$ and m by

$$F_{app} = \frac{1}{1 + \exp\left(\frac{\Delta G_U^{H_2O} - mC}{RT}\right)} \quad (4)$$

The best estimates of $\Delta G_U^{H_2O}$, m, and the midpoint of the unfolding transition, C_M, were obtained by nonlinear least-squares fitting of the data in Figures 4 and 5 to eq 4; these estimates are summarized in Table 1. Since 2.44 M urea corresponds to the C_M of wild-type SNase, the ΔG_U(2.44 M) represents a difference in the stability between mutant and wild-type SNase, denoted by $\Delta\Delta G_U$; this value for each mutant is also shown in Table 1.

The m values of the mutant proteins do not differ remarkably from the value of the wild-type protein, indicating that wild-type and mutant SNase show similar degrees of surface exposure due to unfolding (Table 1). Thus, the structures in both the N and U states of the mutant proteins may not differ remarkably from the corresponding structures of the wild-type proteins. From the $\Delta\Delta G_U$ values, the stabilities $\Delta G_U^{H_2O}$ of all the single mutants of SNase except P56A were identical to that of wild-type SNase, within experimental error. The equilibrium unfolding parameters of the single mutants are in good agreement with those previously reported by Green et al. (*41*), who used intrinsic fluorescence intensity to measure unfolding transitions. All multiple mutants studied here are more stable (0.8−1.3 kcal/mol) than wild-type SNase. This is because all the mutants contain the P117G mutation that is known to increase SNase stability (*30*, *41*). Pro$^-$ is thus significantly more stable than a Pro-minus mutant of SNase studied by Green et al. (*41*). Although the reason for this difference is not clear, the Pro-minus mutant protein is different from SNasePro$^-$ in a residue substituted for Pro. The former does not contain a Thr as a substitute, while the latter contains one Thr at residue 47. Differences in the experimental conditions between the two studies may also be responsible for the above difference.

Refolding Kinetics of Wild-Type and Mutant SNase Measured with Circular Dichroism. For the purpose of investigating the roles of the proline residues in the folding of SNase, kinetic refolding reactions of the wild-type and mutant proteins were initiated by a urea concentration jump from 4.5 to 0.39 M and were assessed by monitoring time-dependent changes in the ellipticity at 225 nm using the stopped-flow CD apparatus, at pH 7.0 (50 mM sodium cacodylate, 50 mM sodium chloride, and 1 mM EGTA) and 20 °C. Because the proteins are fully unfolded at 4.5 M urea

Table 1: Equilibrium Unfolding Parameters of Wild-Type SNase and Its Mutants at pH 7.0 and 20 °C[a]

protein	C_M (M)	m (kcal mol^{-1} M^{-1})	$\Delta G_U^{H_2O}$ (kcal/mol)	$\Delta\Delta G_U$[a] (kcal/mol)
wild-type	2.44 ± 0.02	2.16 ± 0.13	5.30 ± 0.34	−
single mutants				
P11A	2.35 ± 0.01	2.29 ± 0.09	5.38 ± 0.22	−0.21 ± 0.44
P31A	2.34 ± 0.02	2.03 ± 0.01	4.75 ± 0.21	−0.20 ± 0.23
P42A	2.41 ± 0.04	2.33 ± 0.29	5.63 ± 0.75	−0.06 ± 1.45
P56A	2.65 ± 0.02	2.17 ± 0.16	5.77 ± 0.46	0.48 ± 0.85
multiple mutants				
P47T/P117G[b]	3.02 ± 0.01	2.00 ± 0.06	6.04 ± 0.17	1.17 ± 0.05
P11A/P47T/P117G	2.91 ± 0.01	2.17 ± 0.06	6.31 ± 0.18	1.02 ± 0.32
P42P56	2.85 ± 0.01	2.23 ± 0.04	6.35 ± 0.11	0.91 ± 0.20
P56	2.86 ± 0.02	2.02 ± 0.09	5.78 ± 0.26	0.83 ± 0.48
Pro$^-$	3.08 ± 0.01	2.09 ± 0.08	6.43 ± 0.25	1.33 ± 0.44

[a] $\Delta\Delta G_U$ represents the ΔG_U at the urea concentration (2.44 M) where wild-type SNase is half-unfolded. [b] Ref *30*.

Table 2: Kinetic Parameters of the Refolding Reactions of SNase and Its Mutants at pH 7.0 and 20 °C

protein	k_1 (s^{-1})	k_2 (s^{-1})	k_3 (s^{-1})	k_4 (s^{-1})
wild-type	11.4 ± 0.78	1.88 ± 0.051		0.0159 ± 0.00045
wild-type[a]	6.96 ± 0.002	1.86 ± 0.0004		0.017 ± 2.3 × 10^{-6}
single mutants				
P11A	15.6 ± 1.2	1.99 ± 0.033		0.0211 ± 0.0010
P31A	9.61 ± 0.60	1.55 ± 0.043		0.0168 ± 0.00089
P42A	14.9 ± 1.3	2.57 ± 0.13		0.0144 ± 0.00025
P56A	16.7 ± 1.8	2.68 ± 0.082		0.0133 ± 0.00057
multiple mutants				
P47T/P117G	13.6 ± 1.1	2.50 ± 0.25	0.219 ± 0.034	0.0253 ± 0.0013
P11A/P47T/P117G	10.1 ± 0.68	1.94 ± 0.19		0.0339 ± 0.0016
P42P56	8.79 ± 0.59	2.14 ± 0.22		0.0626 ± 0.007
P56	8.66 ± 0.49	1.98 ± 0.28		0.0303 ± 0.0031
Pro$^-$	9.21 ± 0.44	2.09 ± 0.38		

	ellipticity change (deg cm^2 dmol^{-1}) [fractional amplitude (%)][b]				final value (deg cm^2 dmol^{-1})
protein	$\Delta\theta_1$	$\Delta\theta_2$	$\Delta\theta_3$	$\Delta\theta_4$	$\theta(\infty)$
wild-type	−2265 ± 77 (42)	−2336 ± 70 (43)		−796 ± 7 (15)	−9504 ± 53
single mutants					
P11A	−2129 ± 104 (38)	−3116 ± 48 (55)		−413 ± 7 (7)	−9492 ± 49
P31A	−2523 ± 77 (45)	−2472 ± 74 (44)		−599 ± 10 (11)	−10179 ± 50
P42A	−2739 ± 121 (44)	−2558 ± 103 (41)		−913 ± 8 (15)	−10488 ± 80
P56A	−2467 ± 140 (42)	−2891 ± 102 (48)		−656 ± 8 (10)	−10069 ± 78
multiple mutants					
P47T/P117G	−3166 ± 114 (55)	−1649 ± 140 (28)	−406 ± 30 (7)	−582 ± 26 (10)	−9408 ± 48
P11A/P47T/P117G	−3862 ± 138 (70)	−1305 ± 171 (23)		−413 ± 8 (7)	−9078 ± 41
P42P56	−3415 ± 192 (68)	−1469 ± 215 (29)		−177 ± 10 (3)	−9129 ± 49
P56	−3682 ± 160 (78)	−915 ± 183 (19)		−153 ± 7 (3)	−8828 ± 46
Pro$^-$	−4176 ± 143 (87)	−633 ± 168 (13)			−8966 ± 41

[a] The rate constants obtained by fitting a simulation curve based on Scheme 2 to eq 5 (see the Discussion). [b] The fractional amplitude of each phase is shown in parentheses.

and are fully in the N state at 0.4 M urea (Figures 4 and 5), the reaction curves obtained from the urea concentration jump reflect the refolding kinetics from U to N. The data for a series of experiments were fitted by the nonlinear least-squares method to give eq 5

$$\theta(t) = \theta(\infty) + \Delta\theta_{obs}\sum_i \alpha_i e^{-k_i t} = \theta(\infty) + \sum_i \Delta\theta_i e^{-k_i t} \quad (5)$$

where $\theta(t)$ and $\theta(\infty)$ are the observed ellipticity values at time t and infinite time, respectively, $\Delta\theta_{obs}$ is the total observed ellipticity change, and α_i and k_i are the fractional amplitude and the apparent first-order rate constant, respectively, of the ith kinetic phase. The values of $\Delta\theta_i$, α_i, and k_i of all the kinetic phases for wild-type and mutant SNase are listed in Table 2. Three phases were observed for all presently studied proteins except for two SNase mutants, P47T/P117G and Pro$^-$. P47T/P117G shows four phases in the refolding kinetics; it is known to be brought about by the P117G mutation (*30*). SNasePro$^-$, in which all the proline residues are replaced by Ala, Thr, or Gly, shows only the faster two phases, indicating that the slow phase of wild-type SNase is associated with some of the six proline residues (see below). The apparent rate constant for each phase is not affected by the mutations for the proteins that show the three phases, whereas the amplitude ($\Delta\theta_i$) and the fractional amplitude (α_i) of each phase are dependent on the mutation introduced in the protein. In addition to the phases shown in Table 2, there was a burst phase, i.e., an ellipticity change occurring at an early stage of refolding within the dead time of the stopped-flow apparatus; the burst phase amplitude was found to be around 30% of the total ellipticity change expected from the U state to the N state.

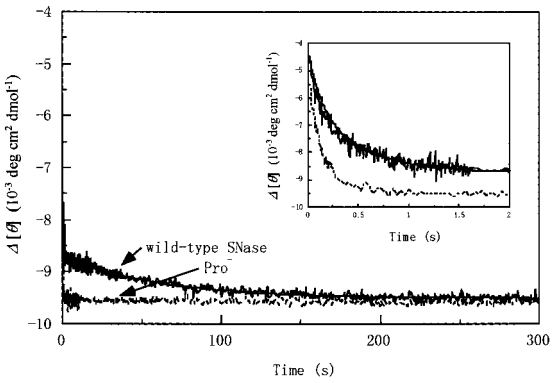

FIGURE 6: Typical kinetic reaction curves of the refolding by urea concentration jump from 4.5 to 0.39 M for wild-type SNase (solid line) and Pro$^-$ (broken line) at pH 7.0 and 20 °C, monitored by CD at 225 nm (50 mM sodium cacodylate, 50 mM sodium chloride, and 1 mM EGTA). The thick solid line shows a time course of the kinetic reaction curve simulated using KINSIM and FITSIM.

(i) Kinetics of Wild-Type SNase. Under the present refolding conditions, wild-type SNase exhibited at least three phases during refolding; the fractional amplitudes of these phases were about 42, 43, and 15% for the fast, the middle, and the slow phases, respectively. These results show that the fast and middle phases were the major phases. The slow phase, which is a minor phase with only 15% of the total amplitude, exhibits a rate constant of 0.0159 s^{-1} typical of the cis−trans isomerizations of the prolyl peptide bonds, and the rate constant is independent of the denaturant concentration (*30*). These results thus strongly suggest that the slow phase is rate-limited by cis−trans isomerizations of prolyl peptide bonds. Non-native proline isomers of SNase may be produced in the U state at equilibrium, and these non-native isomers isomerize into the native isomer at an early stage of refolding, where the protein is still in an intermediate or a denatured state in the native condition (see Discussion and ref *30*). A typical time course for the refolding of wild-type SNase is shown in Figure 6.

(ii) Kinetics of the Single Mutants. Among the four single mutants examined in this study, three (P11A, P31A, and P56A) exhibited refolding kinetics significantly different from the kinetics of wild-type SNase. In these mutants, the amplitude of the slow phase is decreased, although the amplitudes of the faster phases were not considerably affected by the mutations. The extent of the reduction of the slow phase amplitude was 50, 30, and 30% for P11A, P31A, and P56A, respectively, of the corresponding amplitude of wild-type SNase. These results suggest that the slow phase in the refolding kinetics of wild-type SNase can be partly attributed to the three proline residues, Pro^{11}, Pro^{31}, and Pro^{56}.

Nakano and Fink (*29*) also investigated the refolding kinetics of the P31A mutant and reported that the kinetics of the mutant were the same as those of wild-type SNase. Differences in the experimental conditions, such as in temperature and the denaturant used, may be responsible for differences in results. The contribution of Pro^{31} to the slow phase of refolding is also validated from comparison of the kinetics of two multiple mutants (P11A/P47T/P117G and P42P56), in which the replacement of Pro^{31} by Ala is the only difference (Table 1; see below).

In contrast to the three mutants (P11A, P31A, and P56A), the P42A mutant showed refolding kinetics essentially identical to the kinetics of wild-type SNase. This behavior of P42A is very similar to that of the P47T (or P47A) mutant reported in our previous study (*30*), indicating that Pro^{42} and Pro^{47} are not essential in the kinetic refolding of SNase.

(iii) Kinetics of Multiple Mutants. The refolding kinetics of five multiple mutants of SNase, including P47T/P117G, were investigated with stopped-flow CD measurements; the results are summarized in Table 2. As shown in our previous study (*30*), the P47T/P117G mutant shows at least four phases in the refolding process. The appearance of the second-slowest phase (k_3 = 0.22 s^{-1}) in P47T/P117G is known to be due to the P117G mutation, because the P117G mutant shows the same four-phase kinetics. In addition, the P47T mutation does not affect the equilibrium stability or the kinetic refolding of SNase (*30*). However, this second-slowest phase observed in P47T/P117G disappears in the other multiple mutants by the additional mutation (P11A). Comparison of the kinetics between P47T/P117G and P11A/P47T/P117G suggests that Pro^{11} is responsible for the second-slowest phase of P47T/P117G. Thus, there are three phases in the refolding of the three multiple mutants, P11A/P47T/P117G, P42P56, and P56. There are two phases in the refolding of Pro$^-$ that has no proline residues (Table 2). The fractional amplitude of the slow phase decreases with an increase in the number of replaced proline residues. Ultimately, the slow phase is completely eliminated in Pro$^-$. Typical time courses of the refolding of wild-type SNase and Pro$^-$ are compared in Figure 6, which also shows the absence of the slow phase in Pro$^-$. The effects of the replacements of Pro^{42} and Pro^{56} on the slow phase are consistent with those found in the single mutants P42A and P56A. In transition from P42P56 to P56, the P42A mutation does not affect the slow phase amplitude, whereas the P56A mutation of P56 that produces Pro$^-$ eliminates the slow phase of P56. All the above results thus indicate that the slow phase of the refolding of SNase is associated with the proline residues, other than Pro^{42} and Pro^{47}.

Table 2 also shows that the fractional amplitude of the middle phase tends to decrease with an increase in the number of substituted proline residues. Furthermore, the fractional amplitude of the middle phase of Pro$^-$ is only 13%, although it is 43% in wild-type SNase. Thus, the middle phase is also associated with proline residues, although it is not rate-limited by the proline isomerization reaction (see below). However, because Pro$^-$ shows 13% of the fractional amplitude of the middle phase, the portion of the middle phase has no relation to the proline residues.

Refolding Kinetics of Wild-Type SNase in the Presence of E. coli CyPA. The results above indicate that the replacement of certain proline residues decreases the amplitude of the slow and middle phases. To investigate the relationship between these refolding phases, the refolding kinetics of wild-type SNase were investigated in the presence of *E. coli* CyPA (CyPA), which shows PPIase activity. The experimental conditions were the same as those employed above except that the refolding buffer was made from phosphate salts and contained CyPA and DTT. The kinetic parameters obtained at different concentrations of the CyPA are summarized in Table 3, and the CyPA concentration dependence of the kinetic parameters of the individual phases of refolding is

Table 3: Cyclophilin Concentration Dependence of the Refolding Kinetics of Wild-Type SNase at pH 7.0 and 20 °C

CyPA concentration (μM)	apparent rate constant (s^{-1})			ellipticity change[a] (deg cm^2 $dmol^{-1}$)		
	k_1	k_2	k_3	$\Delta\theta_1$	$\Delta\theta_2$	$\Delta\theta_3$
0	9.71 ± 1.41	1.73 ± 0.086	0.017 ± 0.0003	−1799 ± 119 (36)	−2437 ± 153 (49)	−779 ± 6.4 (15)
0.909	9.96 ± 0.74	1.60 ± 0.082	0.026 ± 0.001	−1598 ± 189 (31)	−2781 ± 174 (54)	−736 ± 15.4 (15)
1.62	7.92 ± 0.93	1.57 ± 0.16	0.030 ± 0.001	−3107 ± 253 (51)	−2228 ± 286 (37)	−759 ± 15.6 (16)
2.66	11.90 ± 0.82	1.50 ± 0.07	0.039 ± 0.001	−3436 ± 104 (54)	−2175 ± 103 (34)	−731 ± 11.0 (12)
4.35	12.78 ± 3.34	1.95 ± 0.11	0.062 ± 0.003	−2911 ± 112 (48)	−2346 ± 134 (39)	−816 ± 8.8 (13)

[a] The fractional amplitude of each phase is shown in parentheses.

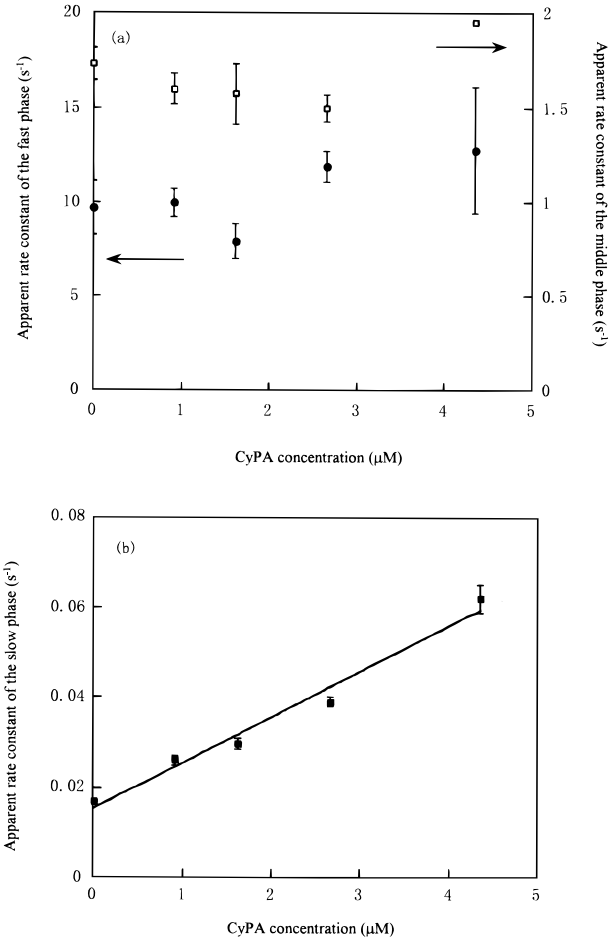

FIGURE 7: CyPA concentration dependence of the refolding rate constants of the (a) fast (●) and middle (□) phases and (b) the slow phase (■). The solid line in panel b shows the result obtained by linear least-squares fitting of the data.

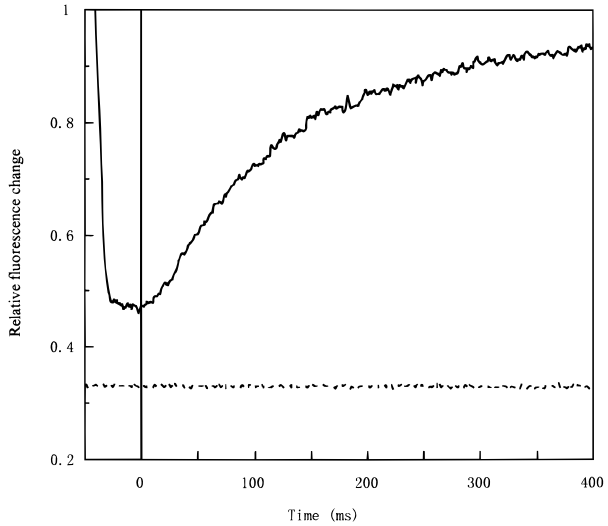

FIGURE 8: Typical kinetic refolding reaction curve caused by a pH jump from pH 1.8 to 6.6 for Pro^- at pH 7.0 and 20 °C (50 mM sodium cacodylate, 50 mM sodium chloride, and 1 mM EGTA), monitored by intrinsic tryptophan fluorescence (solid line). The broken line shows a baseline obtained by mixing of the protein solution at pH 1.8 and the buffer at the same pH value as the protein solution.

illustrated in Figure 7. The apparent rate constant of the slow phase increases with the CyPA concentration, indicating that the slow phase of the refolding reaction is rate-limited by the cis−trans isomerizations of the prolyl peptide bonds and hence is catalyzed by CyPA. However, the apparent rate constants of the fast and middle phases are independent of CyPA concentration (Figure 7). Furthermore, the refolding kinetics of Pro^- in the presence and absence of CyPA were also investigated as a control. CyPA had no effect on both the apparent rate constants and the amplitudes of the refolding (data not shown). These two results indicate that the rates of the fast and middle phases are not limited by proline isomerization.

Refolding Kinetics of SNasePro^- Measured with Tryptophan Fluorescence. The kinetic refolding reactions of Pro^- were also initiated by pH jumps from pH 1.8 to 5.9 and 6.6 (50 mM sodium cacodylate, 50 mM sodium chloride, and 1 mM EGTA) and were measured at 20 °C, by monitoring the changes in tryptophan fluorescence intensity using a stopped-flow fluorescence apparatus. The stopped-flow fluorescence apparatus has a dead time of mixing (3.6 ms) which is much shorter than the dead time of the stopped-flow CD apparatus (23 ms). This renders it useful for investigating earlier stages of the refolding reaction. The measurements were performed at two different protein concentrations, 0.01 and 0.1 mg/mL, and the data were analyzed with eq 5. A typical time course of the refolding kinetics is shown in Figure 8, and the kinetic parameters obtained are summarized in Table 4. The refolding measured by fluorescence was better represented by triphasic kinetics; it exhibited a very fast phase that had an apparent rate constant of 70−200 s^{-1} and showed an opposite change in fluorescence intensity with respect to the changes in the fast and the middle phases of refolding. The rate constants of the fast and the middle phases are in good agreement with those measured with stopped-flow CD, but the very fast phase was too fast to measure with the stopped-flow CD apparatus. Therefore, there must be an intermediate that is formed very rapidly before being detected by the stopped-flow CD apparatus (see the Discussion). By raising the final pH, we increased the apparent rate constants of the three phases, whereas the relative amplitudes were almost

Table 4: pH and Protein Concentration Dependence of the Refolding Kinetics of Pro$^-$ at pH 7.0 and 20 °C

pH	protein concentration (mg/mL)	apparent rate constant (s^{-1}) [fractional amplitude (%)] k_1 (α_1)	k_2 (α_2)	k_3 (α_3)	rms
			18.36 ± 0.45 (0.68 ± 0.01)	4.02 ± 0.13 (0.34 ± 0.12)	12.5
6.6	0.01	214.08 ± 60.5 (−0.21 ± 0.06)	20.80 ± 0.73 (0.66 ± 0.01)	4.34 ± 0.12 (0.34 ± 0.01)	12.2
			9.89 ± 0.21 (0.76 ± 0.01)	1.98 ± 0.13 (0.24 ± 0.02)	6.91
5.9	0.01	70.38 ± 17.3 (−0.13 ± 0.02)	11.51 ± 0.50 (0.72 ± 0.01)	2.34 ± 0.14 (0.28 ± 0.02)	5.55
			9.22 ± 0.073 (0.70 ± 0.01)	1.92 ± 0.050 (0.30 ± 0.01)	13.0
5.9	0.1	107.35 ± 9.34 (−0.12 ± 0.01)	10.33 ± 0.11 (0.73 ± 0.01)	2.27 ± 0.050 (0.27 ± 0.01)	12.5

unchanged. An exception would be the relative amplitude of the very fast phase, which approximately doubled in the transition from pH 5.9 to 6.6. In addition to observations of the very fast phase, there was a burst phase, which showed around 25% of the total fluorescence change in the fluorescence-detected refolding reactions. The refolding kinetics were independent of the final protein concentration, indicating that there was no protein aggregation that affected the kinetics.

DISCUSSION

In this study, the unfolding equilibrium and the refolding kinetics of wild-type SNase, its four single proline mutants (P11A, P31A, P42A, and P56A), and its five multiple mutants (P47T/P117G, P11A/P47T/P117G, P42P56, P56, and Pro$^-$) were studied by CD and fluorescence spectroscopy. The P11A, P31A, and P42A mutations did not change the stability of the protein remarkably, while P56A increases the protein's stability to a small extent, namely, from 0.5 to 0.6 kcal/mol (Table 1). The refolding kinetics of the protein were, however, significantly affected by three of the mutations, namely, P11A, P31A, and P56A. Most notably, the amplitude of the slow phase of refolding decreases with an increase in the number of proline mutations; the amplitude of the middle phase also depends on the number of proline mutations (Table 2). This study considers (1) the effect of the isomerizations of the individual X−Pro peptide bonds on the refolding kinetics and (2) the folding mechanism of SNase probed using the proline mutations.

Effects of the Proline Mutations on the Slow Phase of Refolding. From these results regarding both the single and multiple mutants of SNase (Table 2), three mutations, P11A, P31A, and P56A, decrease the amplitude of the slow phase of refolding, whereas the P42A mutation does not affect slow phase kinetics. These results indicate that the Pro^{11}, Pro^{31}, and Pro^{56} residues are responsible for the slow-folding phase of SNase. The rate constant of the slow phase, 0.01−0.07 s^{-1}, depending on the mutations, is consistent with the isomerization rate of an X−Pro peptide bond of a globular protein. In addition, the refolding kinetics of wild-type SNase in the presence of CyPA show that the apparent rate constant of the slow phase increases with an increase in the concentration of CyPA, and that the slow phase does not contain any portion independent of CyPA (Table 3 and Figure 7). These results thus clearly demonstrate that the entire slow phase is rate-limited by cis−trans isomerizations of the X−Pro peptide bonds. The slow phase rate constant has been shown to be independent of denaturant concentration (*30*), and this is also consistent with the above proposal. Thus, the slow-refolding phase of SNase is schematically represented by Scheme 1

$$I_S \rightleftarrows I_F \rightarrow N$$

where $I_S \rightleftarrows I_F$ represents the slow isomerization between the slow-folding and fast-folding species, I_S and I_F, which correspond to the cis and trans forms, respectively, for the above three X−Pro peptide bonds. I denotes an early intermediate formed within the dead time of the stopped-flow CD apparatus (see below).

When the previous results concerning the SNase mutants with the P117G mutation are taken into account, it is concluded that the slow phase of refolding of SNase is due to the cis−trans isomerizations of the X−Pro peptide bonds, namely, Pro^{11}, Pro^{31}, Pro^{56}, and Pro^{117}. In contrast to the mutations at the above four proline residues, the P42A mutation does not change the slow phase kinetics of refolding (Table 2). Similarly, previous study has shown that the P47T and P47A mutations do not change the equilibrium stability or the refolding kinetics of SNase. Pro^{42} is located in the vicinity of a flexible loop region highly exposed to solvent (residues 43−53) in the native structure of SNase (*24*). Pro^{47} is located within that loop. Eight out of the 11 residues of the loop are hydrophilic. Not only is Thr^{41}, next to Pro^{42}, highly exposed to solvent, but the backbone oxygen of Thr^{41} also maintains a hydrogen bond with a water molecule. The high flexibility and the exposure to solvent of this loop suggest that the refolding could be attained whether the X−Pro peptide bonds of Pro^{42} and Pro^{47} are in the cis form or in the trans form, such that the isomerization of these bonds may not be rate-limiting in the folding reaction. However, the non-native cis isomer of the Thr^{41}−Pro^{42} bond could retard the formation of the native structure (see below).

Effects of the Proline Mutations on the Fast and Middle Phases of Refolding. The apparent rate constants of the fast and middle phases of wild-type SNase refolding are known to increase with a decrease in the final urea concentration. This suggests that these two phases may arise from the structural folding of the protein (*27*, *30*, *31*). The rate constants (>1.5 s^{-1}) of these two phases are too large to be a process rate-limited by the cis−trans isomerization of proline residues. Nevertheless, the amplitude of the middle phase is dependent on the number of proline mutations (Table 2), which indicates that the middle phase is associated with proline residues. In the multiple mutants studied here, at least two mutations, P42A and P56A, reduce the amplitude of the middle phase. In contrast to these results, Veeraraghaven et al. (*33*) reported from their refolding experiments at 2.5 °C that the middle phase rate constant was accelerated by the PPIase. However, the rate constant of the middle phase was decreased from 2 s^{-1} at 20 °C to 0.06 s^{-1} at 2.5 °C, and such a slow reaction at 2.5 °C could be catalyzed by PPIase if the reaction is associated with the cis−trans isomerizations of the prolyl peptide bonds. Therefore, the difference between the results of this study and Veeraraghaven et al. may be due to the difference in the experimental conditions.

When the discussion above is taken into account, the reaction scheme that accounts for these results is thus

rewritten as Scheme 2

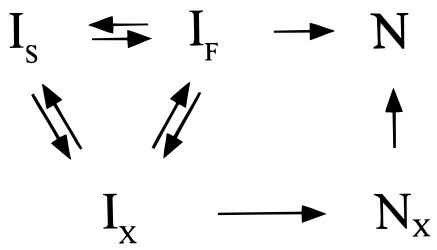

where I_X is an I state that refolds with the rate constant of the middle phase and has at least one non-native proline isomer, provided it is related to proline isomerization. This scheme is consistent with Scheme 4 of our previous study (*30*). It is assumed that in contrast to I_S, I_X refolds to a native-like state, N_X, and the $I_X \rightarrow N_X$ process corresponds to the middle phase of refolding. Although Scheme 2 was first introduced intuitively, the numerical simulations of the reaction kinetics with the use of a computer simulation program, KINSIM (*42*) and FITSIM (*43*), demonstrated that the scheme represents well the observed folding kinetics of wild-type SNase. The thick solid line for the wild-type protein in Figure 6 shows a simulation curve obtained with KINSIM. The fitting of this simulation curve to eq 5 gave the rate constants of refolding sufficiently coincident with those obtained from the observed refolding curve (Table 2). These results indicate that the presence of certain non-native proline isomers may not prohibit folding but rather retard the refolding rate of the protein. A similar result has been reported in the folding of RNase A, in which a native-like state with a non-native trans prolyl bond around Pro^{93} is produced (*12*).

The middle phase, however, does not disappear completely even in Pro^-. The amplitude (13%) of the middle phase is much smaller than the amplitude (43%) for wild-type SNase, but it sufficiently exceeds experimental uncertainty. Thus, the I_X state of Scheme 2 is produced not only by proline isomerization but also by some other conformational event. These results are consistent with a previous study by Walkenhorst et al. (*31*) of the folding kinetics of another Pro-free mutant of SNase in which a fluorescence technique was used. It has been suggested that the isomerization around one or several non-proline peptide bonds leads to the heterogeneity of the U state of SNase and causes the middle phase, although the residues responsible for heterogeneity remain unclear.

Very Fast Phase Detected with Stopped-Flow Fluorescence. To investigate the very early stage of refolding, the refolding reactions of Pro^- were induced by pH jumps from acid to neutral pH values. The kinetics were measured with a stopped-flow fluorescence technique that had a shorter dead time (3.6 ms) than stopped-flow CD. The results reveal that there is a very fast phase with an apparent rate constant of $70-200\ s^{-1}$ and an opposite change in fluorescence intensity with respect to that of the fast and middle phases. The results are consistent with those reported by Walkenhorst et al. (*31*), and this very fast phase may have produced the burst phase intermediates (I_S, I_F, and I_X) observed in the stopped-flow CD experiments. These results also show that the apparent rate constant of this very fast phase is increased with an increase in the final pH, and reaches a value of $200\ s^{-1}$ at pH 6.6. The very fast phase was thus not observed in our stopped-flow CD measurements that were carried out at pH 7 and had a dead time of 23 ms.

Folding Mechanism of SNase Probed by the Proline Mutations. X−Pro peptide bonds of a protein assume both cis and trans isomers in the U state, and the mutation of the proline residues eliminates the cis isomer. As seen above, the isomerizations of certain X−Pro peptide bonds are rate-limiting in the refolding reaction while those of the others are not (*12*). Therefore, the effect of proline mutations on the kinetic refolding will give us an insight into the folding mechanism of SNase. The non-native isomer of an X−Pro peptide bond in the U state may interfere with folding if the X−Pro peptide bond is involved in the native-like structure region of a folding intermediate. However, it may not affect the folding reaction if the X−Pro peptide bond is involved in the unstructured region of the intermediate during the folding. Present and previous results regarding the refolding kinetics of the single mutants of SNase have shown that the mutations of Pro^{11}, Pro^{31}, and Pro^{56} reduce the amplitude of the slow phase of refolding. This suggests that the structures around these three proline residues are organized at an early stage of the refolding of SNase. Although the P117G mutation also affects refolding kinetics, an interpretation of these results may remain unclear because the protein refolds to the N state irrespective of the isomerization state at the Pro^{117} site. On the other hand, the mutations, Pro^{42} and Pro^{47}, do not affect the refolding kinetics of wild-type SNase, which suggests that the structures around these residues may not be organized in the SNase folding intermediate. From the X-ray structure of wild-type SNase (Figure 1), Pro^{11} and Pro^{31} are involved in a major β-sheet core comprised of β-strands 1−3, and Pro^{56} is involved in helix 1, which is adjacent to the β-sheet core. Pro^{42} and Pro^{47} are, however, distinct from the above proline residues and are located around or within the loop comprised of residues 43−53. Thus, these results suggest that the major hydrophobic core formed by the β-strands and helix 1 is important for the folding of SNase and hence is already organized at an early stage of folding. These results are consistent with the hydrogen exchange pulse labeling study of Jacobs and Fox (*44*), in which the intermediate formed after a 5 ms refolding period of SNase shows a modest, yet significant, level of protection for residues in the β-sheet. Although the level of protection of the peptide amide of Ala^{12} is small, the side chains of Glu^{10} and Ala^{12} are incorporated into the hydrophobic core of the β-barrel (*24*). This suggests that the non-native cis isomer of Pro^{11} interferes with the folding of SNase. Our previous study has also shown that the structure around Ala^{69} in helix 1 is organized in the transition state of refolding. This result is consistent with the mutational effect of Pro^{56}, which is also involved in this helix (*45*).

ACKNOWLEDGMENT

We are grateful in particular to Dr. M. M. Dingra for helpful discussion and assistance. We are grateful to Dr. G. P. Tsurupa for her donation of plasmid pMT7-SN-P47T/P117G. We also thank Dr. A. L. Fink for helpful discussion.

REFERENCES

1. Baldwin, R. L. (1975) *Annu. Rev. Biochem. 44*, 453−475.

2. Kim, P. S., and Baldwin, R. L. (1982) *Annu. Rev. Biochem. 51*, 459−489.
3. Kim, P. S., and Baldwin, R. L. (1990) *Annu. Rev. Biochem. 59*, 631−660.
4. Matthews, C. R. (1993) *Annu. Rev. Biochem. 62*, 653−683.
5. Kuwajima, K. (1989) *Proteins 6*, 87−103.
6. Kuwajima, K. (1996) *FASEB J. 10*, 102−109.
7. Kuwajima, K., Hiraoka, Y., Ikeguchi, M., and Sugai, S. (1985) *Biochemistry 24*, 874−881.
8. Ikeguchi, M., Kuwajima, K., Mitani, M., and Sugai, S. (1986) *Biochemistry 25*, 6965−6972.
9. Arai, M., and Kuwajima, K. (1996) *Folding Des. 1*, 275−287.
10. Jennings, P. A., and Wright, P. E. (1993) *Science 262*, 892−896.
11. Brandts, J. F., Halvorson, H. R., and Brennan, M. (1975) *Biochemistry 14*, 4953−4963.
12. Schmid, F. X. (1992) in *Protein folding* (Creighton, T. E., Ed.) W. H. Freeman and Co., New York.
13. Kiefhaber, T., Quaas, R., Hahn, U., and Schmid, F. X. (1990) *Biochemistry 29*, 3053−3061.
14. Kiefhaber, T., Quaas, R., Hahn, U., and Schmid, F. X. (1990) *Biochemistry 29*, 3061−3070.
15. Kiefhaber, T., Grunert, H. P., Hahn, U., and Schmid, F. X. (1990) *Biochemistry 29*, 6475−6480.
16. Jackson, S. E., and Fersht, A. R. (1991) *Biochemistry 30*, 10436−10443.
17. Kiefhaber, T., Kohler, H. H., and Schmid, F. X. (1992) *J. Mol. Biol. 224*, 217−229.
18. Kiefhaber, T., and Schmid, F. X. (1992) *J. Mol. Biol. 224*, 231−240.
19. Schultz, D. A., Schmid, F. X., and Baldwin, R. L. (1992) *Protein Sci. 1*, 917−924.
20. Dodge, R. W., and Scheraga, H. A. (1996) *Biochemistry 35*, 1548−1559.
21. Tan, Y. J., Oliveberg, M., Otzen, D. E., and Fersht, A. R. (1997) *J. Mol. Biol. 269*, 611−622.
22. Tucker, P. W., Hazen, E. J., and Cotton, F. A. (1978) *Mol. Cell Biochem. 22*, 67−77.
23. Loll, P. J., and Lattman, E. E. (1989) *Proteins 5*, 183−201.
24. Hynes, T. R., and Fox, R. O. (1991) *Proteins 10*, 92−105.
25. Fox, R. O., Evans, P. A., and Dobson, C. M. (1986) *Nature 320*, 192−194.
26. Evans, P. A., Dobson, C. M., Kautz, R. A., Hatfull, G., and Fox, R. O. (1987) *Nature 329*, 266−268.
27. Sugawara, T., Kuwajima, K., and Sugai, S. (1991) *Biochemistry 30*, 2698−2706.
28. Kuwajima, K., Okayama, N., Yamamoto, K., Ishihara, T., and Sugai, S. (1991) *FEBS Lett. 290*, 135−138.
29. Nakano, T., Antonino, L. C., Fox, R. O., and Fink, A. L. (1993) *Biochemistry 32*, 2534−2541.
30. Ikura, T., Tsurupa, G. P., and Kuwajima, K. (1997) *Biochemistry 36*, 6529−6538.
31. Walkenhorst, W. F., Green, S. M., and Roder, H. (1997) *Biochemistry 36*, 5795−5805.
32. Schmid, F. X., Mayr, L. M., Muecke, M., and Schoenbrunner, E. R. (1993) *Adv. Protein Chem. 44*, 25−66.
33. Veeraraghavan, S., Nall, B. T., and Fink, A. L. (1997) *Biochemistry 36*, 15134−15139.
34. Pace, C. N. (1986) *Methods Enzymol. 131*, 266−280.
35. Kunkel, T. A. (1985) *Proc. Natl. Acad. Sci. U.S.A 82*, 488−492.
36. Studier, F. W., and Moffatt, B. A. (1986) *J. Mol. Biol. 189*, 113−130.
37. Hayano, T. (1995) Ph.D. Thesis, University of Tokyo, Bunkyo-ku, Tokyo, Japan.
38. Hayano, T., Takahashi, N., Kato, S., Maki, N., and Suzuki, M. (1991) *Biochemistry 30*, 3041−3048.
39. Kuwajima, K., Yamaya, H., Miwa, S., Sugai, S., and Nagamura, T. (1987) *FEBS Lett. 221*, 115−118.
40. Kuwajima, K. (1996) in *Circular dichroism and the conformational analysis of biomolecules* (Fasman, G. D., Ed.) Plenum, New York.
41. Green, S. M., Meeker, A. K., and Shortle, D. (1992) *Biochemistry 31*, 5717−5728.
42. Barshop, B. A., Wrenn, R. F., and Frieden, C. (1983) *Anal. Biochem. 130*, 134−145.
43. Zimmerle, C. T., and Frieden, C. (1989) *Biochem. J. 258*, 381−387.
44. Jacobs, M. D., and Fox, R. O. (1994) *Proc. Natl. Acad. Sci. U.S.A. 91*, 449−453.
45. Kalnin, N. N., and Kuwajima, K. (1995) *Proteins 23*, 163−176.
46. Kraulis, P. J. (1991) *J. Appl. Crystallogr. 24*, 946−950.

BI981962+